PCCP RSCPublishing

ARTICLE

Unique insight on phase separation in polymer solar cells from its electric characteristics

Cite this: DOI: 10.1039/x0xx00000x

Received 00th January 2012,
Accepted 00th January 2012

DOI: 10.1039/x0xx00000x

www.rsc.org/

Jian Wang,[a] Fujun Zhang,[a*] Qiaoshi An,[a] Qianqian Sun,[a] Jian Zhang[b], Bin Hu[a,c*]

A series of polymer solar cells (PSCs) were fabricated with indene-C60 bisadduct (ICBA) or [6,6]-phenyl-C61-butyric acid methyl ester ($PC_{61}BM$) as electron acceptor and with PBDT-TS1 as electron donor. The donor/acceptor (D/A) phase separation was adjusted with different solution processing methods, consisting of cool (room temperature, 20 ºC) solution, hot (70 ºC) solution and the solutions with solvent additive 1,8-diiodideoctane (DIO). The champion PCE of PSCs with ICBA or $PC_{61}BM$ as electron acceptor is 4.32% or 5.97% for the active layers prepared from hot solution with DIO additive or cool solution with DIO additive, respectively. The improved PCEs should be attributed to the optimized D/A phase separation in the active layers by adjusting the redistribution of $PC_{61}BM$ or ICBA among the PBDT-TS1 networks. The degree of phase separation of the active layers with different acceptors was evaluated according to the current density-voltage (*J-V*) curves of hole-only and electron-only devices. The distribution of $PC_{61}BM$ or ICBA molecules in the normal direction can be simply judged from the symmetry degree of *J-V* curves of electron-only devices measured under the forward and reverse bias.

Introduction

Polymer solar cells (PSCs) have attracted much attention due to the unique advantages such as low cost, flexibility and environmentally-friendly process [1-3]. Up to now, the power conversion efficiency (PCE) of bulk heterojunction PSCs has been improved to ~ 10% by different strategies from material synthesis or device physics [4, 5]. Among the approaches in increasing the PCE of PSCs, optimizing donor/acceptor (D/A) phase separation in the active layers plays the critical role. The gradual vertical D/A phase separation with acceptor-rich materials in the region near the cathode and donor-rich materials in the region near the anode is beneficial to improve charge collection and thus PCE of PSCs [6, 7]. In order to understand and better optimize the D/A phase separation, many technologies have been employed to investigate the active layers, including: i) estimating the surface composition by energy dispersive spectrometer (EDS), X-ray photoelectron spectroscopy (XPS), peak force Kelvin ProbeForce microscopy (PF-KPFM) and water contact angle (WCA) characterization [6, 8]; ii) characterizing the concentration-depth profiles with spectroscopic ellipsometry (SE), cross-sectional scanning tunneling microscope (XSTM) and secondary ion mass spectroscopy (SIMS) [9-12]; and iii) quantizing the degree of phase separation with resonant soft-X-ray scattering (R-SoXS) [13]. Though these technologies have unique superiority in investigating the D/A phase separation, the rigorous technology requirements and high cost limit their popular application. Hence, simple and effective methods are needed to clearly evaluate the degree of D/A phase separation dependence on the chemical structure of fullerene derivations and preparing conditions of active layers.

In 2010, Li et al. successfully reported the electron acceptor indene-C60 bisadduct (ICBA), which may increase the open-circuit voltage (V_{OC}) and PCE of PSCs by replacing the widely used [6,6]-phenyl-C61-butyric acid methyl ester ($PC_{61}BM$) or [6,6]-phenyl-C71-butyric acid methyl ester ($PC_{71}BM$) [14, 15]. However, the PSCs based on narrow bandgap polymer/ICBA active layers usually show rather low short circuit current (J_{SC}) and fill factor (FF) [16, 17]. Li's group and Yang's group respectively pointed out that the PCE of PSCs based on narrow bandgap polymer and ICBA may be mainly limited by large D/A phase separation in the active layers [18, 19]. It is known that the degree of D/A phase separation should be mainly determined by the distribution of electron acceptor molecules among the polymer networks [6, 20, 21]. It means that the degree of D/A phase separation can be evaluated from the electron transport behavior in the active layers. Recently, Hou et al. reported that the $PC_{71}BM$ molecules may diffuse towards the top surface of active layers along with the elevated volatilization of solvent or solvent additive [8]. Zhang et al. reported that the low PCE of PSCs with ICBA as electron acceptor may be attributed to the limited molecular distribution of ICBA among donor materials resulted from its symmetric molecular structure [22]. Hence, the improved vertical D/A phase separation in the active layers consisting of narrow bandgap polymer donor and ICBA acceptor may be the important factor for the low J_{SC} and FF of the related PSCs.

In this work, a series of PSCs were prepared with narrow bandgap polymer PBDT-TS1 as electron donor and with ICBA or $PC_{61}BM$ as electron acceptor. The degree of D/A phase separation can be adjusted by using different temperature solutions and solvent additive. For the PSCs with PBDT-TS1:ICBA (1:1.5, wt/wt) as active layer, the PCE was increased from 3.25% to 4.32% by employing hot (70 °C) solution with DIO additive. For the PSCs with PBDT-TS1:$PC_{61}BM$ (1:1.5, wt/wt) as active layer, the PCE was increased from 5.56% to 5.97% by preparing the active layer from cool (room temperature) solution with DIO additive. The improved PCEs should be attributed to the optimization of D/A phase separation in the active layers, which can be evaluated from the *J-V* curves of the corresponding electron-only devices. It is worth highlighting that the optimization of vertical D/A phase separation due to the migration of ICBA or $PC_{61}BM$ molecules towards the top surface of active layers can be evaluated from the symmetry degree of *J-V* curves of electron-only devices under forward or reverse bias. Compared with the PSCs with PBDT-TS1:$PC_{61}BM$ as active layer, the lower performance of PSCs based on PBDT-TS1:ICBA mainly resulted from the discontinuous electron transport channels due to the aggregation of ICBA. The electric character of active layers obtained from the *J-V* curves of the hole-only and electron-only devices according to the PSCs may provide a unique insight on the relative D/A phase separation degree in the active layers with different acceptors.

2 Experimental details

2.1 Preparation of the samples

Patterned indium tin oxide (ITO) coated glass substrates (15 $\Omega/\square$) were consecutively cleaned by glass lotion, de-ionized water and ethanol in ultrasonic baths, followed by the stoving-dried and UV-O_3 treatment for 6 minutes. Poly(3,4-ethylenedioxythiophene):poly(styrenesulfonate) (PEDOT:PSS, Clevios AI 4083) was spin-coated onto the ITO coated substrates at 5000 rounds per minute (RPM) for 40 s. Then the PEDOT:PSS coated ITO substrates were annealed at 120 °C for 10 minutes in atmospheric air environment and transferred into a high purity nitrogen filled glove box. The electron donor PBDT-TS1 and electron acceptor ICBA or $PC_{61}BM$ were dissolved in 1,2-dichlorobenzene (*o*-DCB) to prepare the blend solutions with a concentration of 25 mg/mL, the D/A weight ratio was kept constant at 1:1.5 for the solutions. Part of blend solutions were added 3% (v/v) solvent additive 1,8-diiodideoctane (DIO) to adjust electron acceptor aggregation extent in the blend films with continuously stirring. Then part of blend solutions were heated to 70 °C with continuously stirring to further increase mixing degree of electron donor and acceptor. The blend solutions were spin-coated onto the PEDOT:PSS coated substrates to prepare the active layers at 1000 RPM for 40 s. All blend films were placed in vacuum condition (~ 1 Pa) for 10 minutes to accelerate dry speed of active layer and decrease the residual DIO in the active layers. The semiconducting conjugated polyelectrolyte poly[9,9-bis(3'-(N,N-dimethylamino) -propyl-2,7-fluorene)-alt-2,7-(9,9-dioctylfluorene)] (PFN) was dissolved in methanol to prepare 0.2 mg/ml solution with addition of 0.25 vol% acetic acid, and then PFN solutions were spin-coated on the top of active layers at 3000 RPM for 30 s to prepare the interfacial buffer layer. The aluminum (Al), silver (Ag), molybdenum oxide (MoO_3) or lithium fluoride (LiF) was deposited by thermal evaporation under 3×10^{-4} Pa vacuum conditions. The thickness of films was monitored by using a quartz crystal microbalance. The active area of each cell is about 3.8 mm^2, which is defined by the overlap of ITO anode and Al cathode. All the measurements were carried out in ambient conditions.

2.2 Characterizations

The current density-voltage (*J-V*) characteristics of PSCs were measured by a Keithley 4200 semiconductor characterization system in dark and under light conditions. AM 1.5 illumination at 100 mW/cm^2 was provided by an ABET Sun 2000 solar simulator. The external quantum efficiency (EQE) spectra of PSCs were measured by a Zolix Solar Cell Scan 100. Absorption spectra of neat or blend films were measured with a Shimadzu UV-3101 PC spectrophotometer. Photoluminescence (PL) spectra of films were measured by using a HORIBA Fluorolog®-3 Spectrofluorometer. The morphology and phase images of active layers were investigated by using atomic force microscopy (AFM) with a multimode Nanoscope IIIa operated in tapping mode. The chemical structure, highest occupied molecular orbital (HOMO) and lowest unoccupied molecular orbital (LUMO) levels of used materials are shown in Fig. 1.

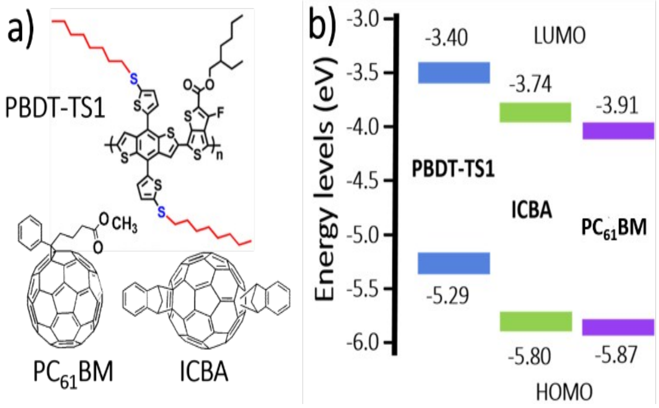

Fig. 1 (a) The chemical structure and (b) energy level diagram of PBDT-TS1, ICBA and $PC_{61}BM$.

3 Results and discussion

The absorption spectra of PBDT-TS1, ICBA and $PC_{61}BM$ films were measured and are shown in Fig. 2. The PBDT-TS1 film exhibits a relatively broad absorption range with an absorption peak at about 722 nm and a shoulder peak at about 657 nm. The HOMO and LUMO levels of PBDT-TS1 are about -5.29 eV and -3.40 eV, corresponding to a 1.89 eV bandgap [23]. Both ICBA and $PC_{61}BM$ exhibit very similar absorption intensity in the whole spectral range. It is envisaged that all the blend films should have the same absorption intensity and range, which is confirmed form the absorption spectra of the blend films prepared with different solutions, as shown in Fig. S1. It means that the photon harvesting ability should be the same for all PSCs with PBDT-TS1:ICBA or PBDT-TS1:$PC_{61}BM$ as the active layer. Therefore, the effect of $PC_{61}BM$ or ICBA on the J_{SC} and FF should be mainly attributed to the different D/A phase separation degree in the active layers. It is known that the open circuit voltage (V_{OC}) is mainly determined by the energy offset between the HOMO level of electron donor and LUMO level of electron acceptor for PSCs with the same interfacial layers and electrodes [24]. The LUMO-LUMO offsets between PBDT-TS1 and ICBA or $PC_{61}BM$ are about 0.34 and 0.51 eV, which are larger than the typical value 0.3 eV for providing enough driving force for efficient exciton dissociation [25].

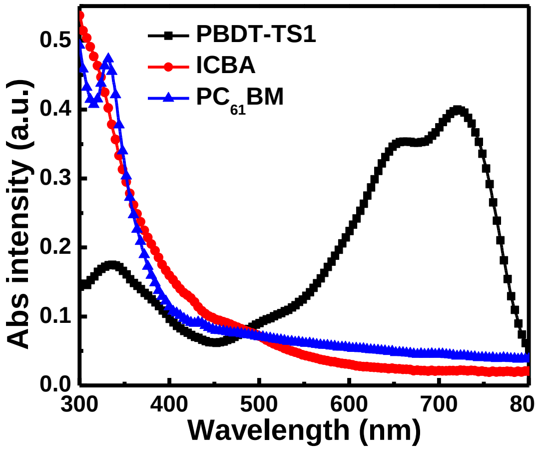

Fig. 2 The absorption spectra of PBDT-TS1, ICBA and $PC_{61}BM$ films.

The variation of D/A phase separation should be mainly attributed to ICBA or $PC_{61}BM$ molecules redistribution in polymer matrix during film drying process. The blend solution conditions (temperature, DIO additive) should result in the different phase separation extent due to the different film drying process. The active layers prepared from hot (70 ^{o}C) solutions can be considered as the fast forming films process, D/A molecular distribution in solution states may be rapidly fixed in the solid films. The active layers prepared from cool solution and cool solution with DIO additive can be considered as the slow film drying processes, the ICBA or $PC_{61}BM$ molecular may redistribute or migrate along with the volatilization of solvent or DIO additive from the wet films. Meanwhile, the chemical structure of ICBA or $PC_{61}BM$ may also influence its molecular redistribution during film drying process.

For PSCs with ICBA as electron acceptor, the *J-V* characteristic curves and EQE spectra of PSCs prepared from the different solutions were measured and are shown in Fig. 3.

More than one hundred PSCs were prepared to confirm the solution processing methods on PSCs performance, the detailed *J-V* curves are shown in Fig. S2. The key parameters of PSCs were summarized and are listed in Table 1. All the PSCs with ICBA as electron acceptor exhibit a relatively large V_{OC} of 1.02 V, which can be well explained from the relatively high LUMO level of ICBA. The PCEs of PSCs prepared from cool solution were increased from 3.25% to 4.16% by doping DIO additive, the PCE improvement should be attributed to the more ICBA diffusion to the top surface of active layers during the volatilization of DIO additive, which can be further confirmed form the increased FF from 40.2% to 45.1%. The PSCs prepared from hot solution also exhibit the better performance compared with the PSCs prepared from cool solution, which should be attributed to more homogenous D/A distribution in the active layers due to the relatively fast film drying process. For the active layers prepared from cool solution without DIO additive, ICBA may tend to aggregate in the active layers, rather than diffuse toward the top surface of active layers due to the absent driving force induced by the volatilization of DIO additive. The champion PCE of PSCs arrived to 4.32% for the active layers prepared from the hot solution with DIO additive, the better vertical phase separation of PBDT-TS1:ICBA should be obtained because more ICBA can be elevated toward the top surface of active layers during volatilization of solvent and solvent additive DIO. The more ICBA near top surface of active layers is beneficial to decrease the series resistance (R_S) and increase FF. The optimized PSCs exhibit the smallest R_S of 25 Ω/cm^2 and the best FF of 48.3% for the active layers prepared from hot solutions with DIO additive. The R_s was decreased from 45 to 25 Ω/cm^2 and shunt resistance (R_{SH}) was increased from 583 to 841 Ω/cm^2 by adjusting phase separation, resulting in the increased FF from 40.2% to 48.3%. This phenomenon further indicates that the vertical phase separation can be optimized by elevating ICBA toward the top surface of active layers during film drying process.

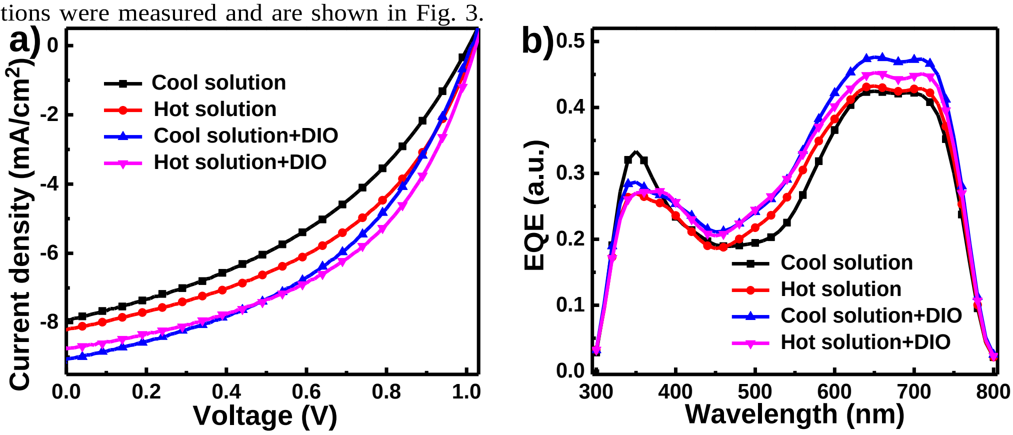

Fig. 3 (a) *J-V* curves of PSCs under AM 1.5 illumination at 100 mW/cm^2 and (b) EQE spectra of PSCs based on ICBA as electron acceptor with the active layers prepared from different solution conditions.

Table 1. The key photovoltaic parameters of PSCs prepared with ICBA as electron acceptor

Solutions	V_{oc} (V)	J_{sc} (mA/cm^2)	FF (%)	Best PCE (%)	Ave PCE (%)	R_s (Ω/cm^2)	R_{sh} (Ω/cm^2)
Cool	1.02	7.92	40.2	3.25	3.11 (±0.12)	45	586
70 ^{o}C	1.02	8.21	44.6	3.73	3.58 (±0.15)	32	712
DIO	1.02	9.05	45.1	4.16	3.90 (±0.25)	28	583
70 ^{o}C + DIO	1.02	8.76	48.3	4.32	4.20 (±0.10)	25	841

Average PCEs were calculated based on 20 cells.

For the PSCs with $PC_{61}BM$ as electron acceptor, the *J-V* characteristic curves and EQE spectra of PSCs were measured and are shown in Fig. 4. More than one hundred PSCs were prepared by using different solutions and the detailed *J-V* curves of part cells are shown in Fig. S3. The key photovoltaic parameters of PSCs were summarized according to *J-V* curves and are listed in Table 2. The champion PCE of PSCs with $PC_{61}BM$ as electron acceptor was 5.97% for the active layers prepared from cool solution with DIO additive, along with a relatively high J_{SC} of 11.50 mA/cm^2 and a FF of 62.5% as well as a V_{OC} of 0.83 eV. For the active layers prepared from cool solution with DIO additive, more $PC_{61}BM$ can be elevated towards the top surface of active layers during the relatively slow drying process. The asymmetric structure of $PC_{61}BM$ may be beneficial to molecular diffusion under the driving force induced by the volatilization of solvent or DIO additive. The PSCs with $PC_{61}BM$ as electron acceptor exhibit the smaller R_S and the larger R_{SH} compared with PSCs with ICBA as electron acceptor, indicating that the $PC_{61}BM$ molecules can be easily elevated toward the top surface of active layers compared with ICBA molecules. The better FF and J_{SC} of PSCs with $PC_{61}BM$ as electron acceptor indicate that the degree of vertical phase separation formed in the active layers is more beneficial to the exciton dissociation, charge carrier transport and collection.

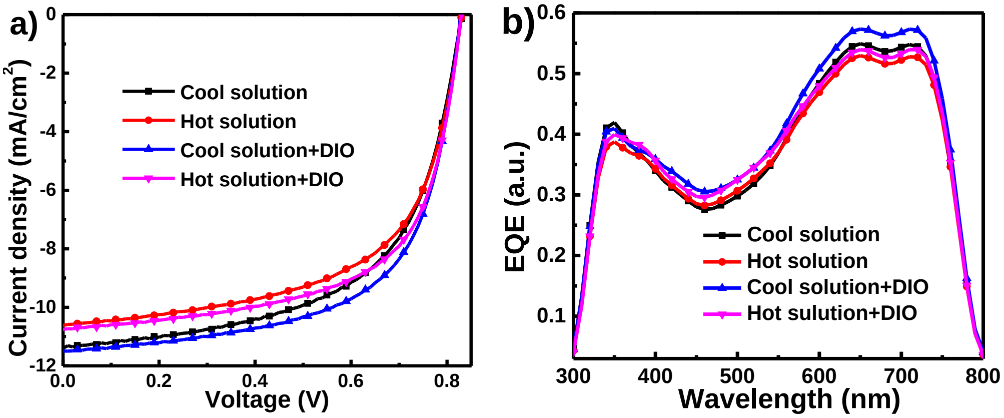

Fig. 4 (a) *J-V* curves of PSCs under AM 1.5 illumination at 100 mW/cm^2 and (b) EQE spectra of the PSCs with $PC_{61}BM$ as electron acceptor.

Table 2. The key photovoltaic parameters of PSCs prepared with $PC_{61}BM$ as electron acceptor

Solutions	V_{oc} (V)	J_{sc} (mA/cm^2)	FF (%)	Best PCE (%)	Ave PCE (%)	R_s (Ω/cm^2)	R_{sh} (Ω/cm^2)
Cool	0.83	11.40	58.8	5.56	5.45 (±0.08)	8.9	605
70 °C	0.83	10.62	60.1	5.30	5.26 (±0.03)	8.8	822
DIO	0.83	11.50	62.5	5.97	5.84 (±0.11)	7.4	1288
70 °C + DIO	0.83	10.75	62.8	5.60	5.48 (±0.10)	7.3	1318

Average PCEs were calculated based on 20 cells.

For better understand the effect of phase separation degree on exciton dissociation, the photoluminescence (PL) spectra of neat PBDT-TS1 film, PBDT-TS1:ICBA and PBDT-TS1:$PC_{61}BM$ blend films prepared from different solutions were measured under the excitation of 680 nm light, as shown in Fig. S4. The typical PL spectra of neat PBDT-TS1 and the corresponding blend films are shown in Fig. 5. It is apparent that neat PBDT-TS1 films exhibit strong PL emission with emission peak at 790 nm. The PL emission of PBDT-TS1 is almost completely quenched in the all PBDT-TS1:$PC_{61}BM$ blend films, exhibiting the homogeneous D/A molecular distribution in the blend films. However, the PL emission of PBDT-TS1 is partly quenched in the PBDT-TS1:ICBA blend films prepared from cool solution, which may be due to the serious aggregation of ICBA during the slow drying process of films. The emission of PBDT-TS1 was markedly quenched for the PBDT-TS1:ICBA blend films prepared from hot solution with DIO additive, exhibiting the limited ICBA aggregation during the rapid drying process. The observed from the PL spectra of active layers indicates that ICBA molecules may prefer to aggregate in the blend films resulting in the relatively strong PBDT-TS1 emission, which can effectively explain the performance of PSCs dependence on the active layers prepared from different solution conditions.

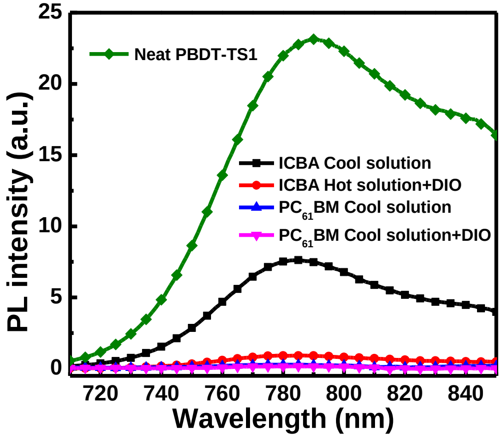

Fig. 5 PL spectra of neat PBDT-TS1, PBDT-TS1:ICBA and PBDT-TS1:$PC_{61}BM$ blend films prepared from different solution conditions.

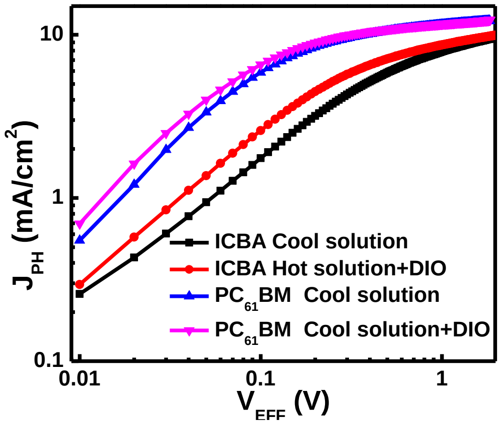

Fig. 6 The J_{PH}-V_{EFF} curves of PSCs with PC$_{61}$BM or ICBA as electron acceptor.

To further investigate the effect of phase separation degree on the exciton dissociation and charge carrier transport in the active layers, the photocurrent density (J_{PH}) versus effective voltage (V_{EFF} = V_0-V) curves of PSCs were calculated according to the *J-V* curves in dark and under AM 1.5 illumination at 100 mW/cm^2, as shown in **Fig. 6**. The J_{PH} is defined as the difference between the current density under illumination (J_L) and the current density in the dark (J_D), thus J_{PH} = J_L - J_D. V_o is the voltage at which J_{PH} = 0 and *V* is the applied bias voltage [26]. It is apparent that the J_{PH} of PSCs based on PBDT-TS1:PC$_{61}$BM as the active layer rapidly come into the saturation state under relatively low V_{EFF} compared with that of PSCs based PBDT-TS1:ICBA as the active layer, which indicates the more efficient charger carrier transport channels formed in the PBDT-TS1:PC$_{61}$BM blend films. The saturation current density (J_{SAT}) of PSCs with PC$_{61}$BM as electron acceptor is about 12 mA/cm^2 at V_{EFF} = 2 V, which is larger than that of 10 mA/cm^2 for the PSCs with ICBA as electron acceptor. The exciton dissociation probability and charge carriers collection could be deduced from J_{PH}/J_{SAT} under short circuit condition and maximum power output conditions [27, 28]. Under short circuit condition, the J_{PH}/J_{SAT} is about 94% or 88% for PSCs with PC$_{61}$BM or ICBA as electron acceptor, indicating high exciton dissociation efficiency which well accords with the PL emission quenching extent of the corresponding blend films. At the maximum power output conditions, the J_{PH}/J_{SAT} is about 75% or 62% for PSCs with PC$_{61}$BM or ICBA as electron acceptor, which indicates the lower charge carriers transport and collection ability in the PBDT-TS1:ICBA active layer. It also well accords with the relative FF of corresponding PSCs with ICBA as acceptor.

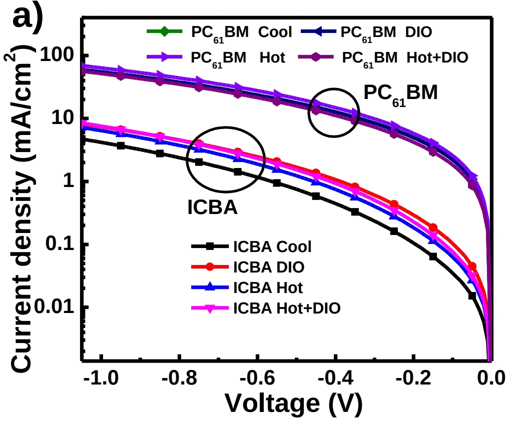

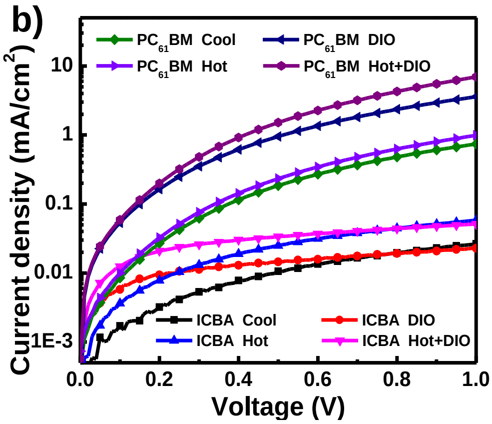

Fig. 7 The *J-V* characteristic curves of the (a) hole-only and (b) electron-only devices.

The hole-only ITO/PEDOT:PSS/active layers/MoO$_3$ (10 nm)/Ag (50 nm) and electron-only Al (100 nm)/LiF (1 nm)/active layers/LiF (1 nm)/Al (100 nm) devices were fabricated to investigate the charge carrier transport of active layers prepared different solution conditions. The *J-V* curves of the hole-only and electron-only devices were measured in dark conditions and are shown in Fig. 7. To provide more valuable information on the charge carrier transport ability in the PSCs, charge carrier transport characteristics of hole-only or electron-only devices were investigated under forward (hole collected by ITO cathode) or reverse (electron collected by top Al cathode) bias. It is apparent that hole and electron transport ability of devices based on PBDT-TS1:PC$_{61}$BM as the active layer are larger than those of devices based on PBDT-TS1:ICBA as the active layer, which indicates that the better bicontinuous charge carrier transport channels have been formed in the devices with PBDT-TS1:PC$_{61}$BM as the active layer. It should be highlighted that hole transport ability of all devices is stronger than the corresponding electron transport ability, indicating that the performance of PSCs may be limited by the unbalanced charge transport due to the relatively low electron transport ability in the active layers. Hole transport ability of blend films is insensitive to the film drying process, as shown in Fig. 7a, indicating a relatively stable network of polymer. Meanwhile, hole transport ability in the PBDT-TS1:ICBA blend films was markedly decreased due to the aggregation of ICBA. According to the Fig. 7b, electron transport ability of active layers is more sensitive to the film drying process due to the easy redistribution of small molecules ICBA or PC$_{61}$BM in the active layers during film drying process. The relatively larger electron transport ability of PBDT-TS1:PC$_{61}$BM blend films should be beneficial to the more balanced charge transport in the active layer, resulting in the relatively high performance of the PSCs with PBDT-TS1:PC$_{61}$BM as the active layer. The relatively weak electron transport ability of PBDT-TS1:ICBA blend films may be due to discontinuous electron transport channels due to the aggregation of ICBA. To further investigate ICBA or PC$_{61}$BM distribution in the active layers, *J-V* curves of the electron-only devices (Al (100 nm)/LiF (1 nm)/active layers/LiF (1 nm)/Al (100 nm)) were measured under forward bias or reverse bias and the description is shown in Fig. 8a. Under the forward bias, electrons are injected from the bottom Al electrode. Under the reverse bias, electrons will be injected from the top Al electrode. According to the energy levels of used materials shown in Fig. 8b, the electron can be relatively easily injected from Al electrode onto the LUMO of ICBA or

$PC_{61}BM$ if more ICBA or $PC_{61}BM$ molecules enriched near the top surface of the active layers [29].

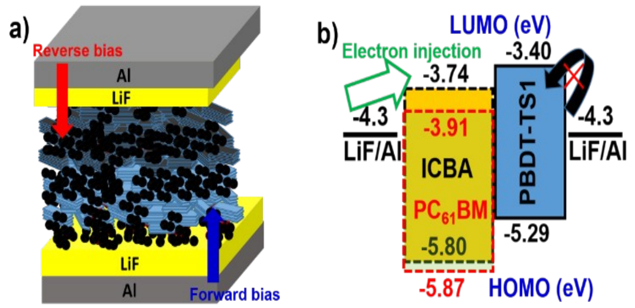

Fig. 8 (a) The schematic diagram of electron injection under the forward or reverse bias, (b) the energy level diagram of used materials

The double-logarithmic *J-V* curves of the electron-only devices measured in dark are shown in Fig. 9a and 9b, as well as the single-logarithmic *J-V* curves in inserted images. It is apparent that the *J-V* curves of devices with PBDT-TS1:$PC_{61}BM$ as active layer exhibit a similar characteristics under forward and reverse bias, it means that the distribution of $PC_{61}BM$ neat top or bottom surface of active layer should be same. However, the *J-V* curves of devices with PBDT-TS1:ICBA as active layer exhibits a distinct deviation under forward and reverse bias, indicating that the distribution of ICBA near top or bottom surface of active layer should be obviously different. For the blend films, the redistribution of ICBA and $PC_{71}BM$ can be effectively optimized by using different solution conditions to form the better vertical phase separation in the active layers. The *J-V* curves of the symmetric electron-only devices under forward or reverse bias were investigated, which may be a simple and effective method to evaluate the vertical phase separation in the active layers.

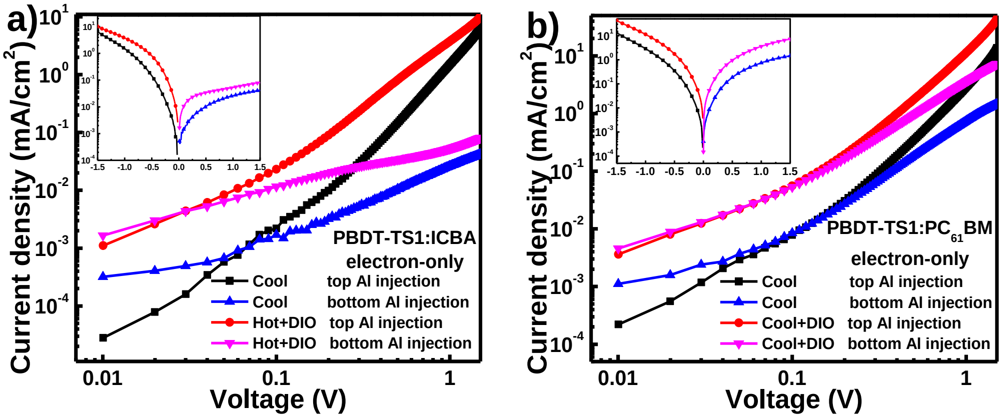

Fig. 9 The double-logarithmic *J-V* curves of devices with (a) PBDT-TS1:ICBA, (b) PBDT-TS1:$PC_{61}BM$ as the active layer under forward or reverse bias.

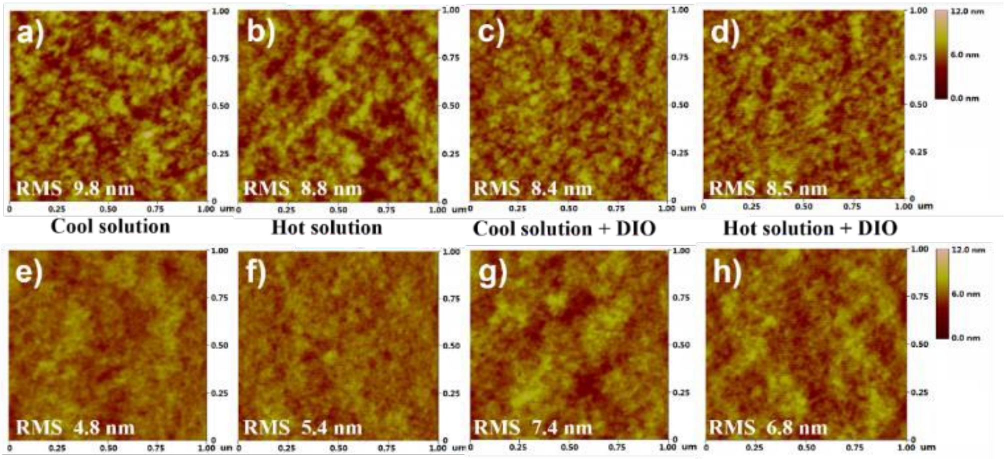

Fig. 10 Morphology images of (a-d) PBDT-TS1:ICBA and (e-h) PBDT-TS1:$PC_{61}BM$ blend films.

As we can envisage, the variation of phase separation may be slightly reflected by the surface morphology of active layer. The morphology of all active layers with different electron acceptor or prepared from different solution conditions was characterized by atomic force microscopy (AFM), as shown in Fig. 10. The corresponding phase images of active layers are shown in Fig. S5. The surface root mean square (RMS) roughness of the PBDT-TS1:ICBA blend films are much larger than that of PBDT-TS1:$PC_{61}BM$ blend films, which may be due to ICBA aggregation in the active layers. Meanwhile, the surface roughness of active layers strongly depends on the corresponding solution conditions, which also indirectly reflects the degree of phase separation in the active layers. To intuitively investigate the redistribution of ICBA or $PC_{61}BM$ on the phase separation, a schematic image of phase separation of active layer with different film drying process is shown in the Fig. S6. The D/A phase separation strongly depends on the solution conditions, post treatment conditions on the active layer as well as the intrinsic factors of electron donor and electron acceptor molecular chemical structures.

4 Conclusions

In summary, the champion PCE values of PSCs arrived to 4.32% or 5.97% for the cells with ICBA or $PC_{61}BM$ as electron acceptor and PBDT-TS1 as electron donor, respectively. The PCE of PSCs based on PBDT-TS1:ICBA was increased from 3.25% to 4.32% by optimizing the D/A phase separation with hot solution and solvent additive DIO. The PCE of PSCs based on PBDT-TS1:$PC_{61}BM$ was increased from 5.56% to 5.97% by preparing the active layers with solvent additive DIO. The PL spectra shows that the exciton dissociation efficiency in PBDT-TS1:ICBA can be increased by decreasing ICBA aggregation level and optimizing ICBA distribution in the active layer. The *J*-*V* curves of related hole-only and electron-only devices indicate that enhanced and more balanced charge transport ability can be obtained by optimizing D/A phase separation. The photovoltaic parameters of PSCs can be purposely optimized by adjusting solution conditions according to the chemical structures of electron donor and electron acceptor. The investigation on *J*-*V* curves of the symmetric electron-only devices under forward or reverse bias may provide a simple and effective method to evaluate the vertical phase separation in the active layers.

Acknowledgements

This work was supported by the Fundamental Research Funds for the Central Universities (2015YJS182), National Natural Science Foundation of China (61377029), and Beijing Natural Science Foundation (2122050).

Notes and references

[a] Key Laboratory of Luminescence and Optical Information, Ministry of Education, Beijing Jiaotong University, Beijing 100044, China E-mail: fjzhang@bjtu.edu.cn

[b] Department of Material Science and Technology, Guangxi Key Laboratory of Information Materials, Guilin University of Electronic Technology, Guilin 541004, Guangxi, China

[c] Department of Materials Science and Engineering, University of Tennessee, Knoxville, Tennessee 37996, United States E-mail: bhu@utk.edu

† Electronic Supplementary Information (ESI) available. See DOI: 10.1039/b000000x/

1. F. C. Krebs, N. Espinosa, M. Hösel, R. R. Søndergaard and M. Jørgensen, *Adv. Mater.*, 2014, **26**, 29-39.

2. R. Po, A. Bernardi, A. Calabrese, C. Carbonera, G. Corso and A. Pellegrino, *Energy Environ. Sci.*, 2014, **7**, 925-943.

3. F. C. Krebs, *Sol. Energy Mater. Sol. C.*, 2009, **93**, 394-412.

4. Y. Liu, J. Zhao, Z. Li, C. Mu, W. Ma, H. Hu, K. Jiang, H. Lin, H. Ade and H. Yan, *Nat. Commun.*, 2014, **5**. 5293.

5. J.-D. Chen, C. Cui, Y.-Q. Li, L. Zhou, Q.-D. Ou, C. Li, Y. Li and J.-X. Tang, *Adv. Mater.*, 2015, **27**, 1035-1041.

6. X. Guo, M. Zhang, W. Ma, L. Ye, S. Zhang, S. Liu, H. Ade, F. Huang and J. Hou, *Adv. Mater.*, 2014, **26**, 4043-4049.

7. L. Zhang, X. Xing, L. Zheng, Z. Chen, L. Xiao, B. Qu and Q. Gong, *Sci. Rep.*, 2014, **4**, 5071.

8. L. Ye, Y. Jing, X. Guo, H. Sun, S. Zhang, M. Zhang, L. Huo and J. Hou, *J. Phys. Chem. C*, 2013, **117,** 14920-14928.

9. R. Kokubu and Y. Yang, *Phys. Chem. Chem. Phys*., 2012, **14**, 8313-8318.

10. M.-C. Shih, B.-C. Huang, C.-C. Lin, S.-S. Li, H.-A. Chen, Y.-P. Chiu and C.-W. Chen, *Nano Lett.*, 2013, **13**, 2387-2392.

11. M. Campoy-Quiles, T. Ferenczi, T. Agostinelli, P. G. Etchegoin, Y. Kim, T. D. Anthopoulos, P. N. Stavrinou, D. D. C. Bradley and J. Nelson, *Nat. Mater*., 2008, **7**, 158-164.

12. J. Liu, Q. Liang, H. Wang, M. Li, Y. Han, Z. Xie and L. Wang, *J. Phys. Chem. C*, 2014, **118**, 4585-4595.

13. W. Ma, J. R. Tumbleston, L. Ye, C. Wang, J. Hou and H. Ade, *Adv. Mater*., 2014, **26**, 4234-4241.

14. Y. He, H.-Y. Chen, J. Hou and Y. Li, *J. Am. Chem. Soc.*, 2010, **132**, 1377-1382.

15. M. A. Faist, S. Shoaee, S. Tuladhar, G. F. A. Dibb, S. Foster, W. Gong, T. Kirchartz, D. D. C. Bradley, J. R. Durrant and J. Nelson, *Adv. Energy Mater*., 2013, **3**, 744-752.

16. T. E. Kang, H.-H. Cho, C.-H. Cho, K.-H. Kim, H. Kang, M. Lee, S. Lee, B. Kim, C. Im and B. J. Kim, *ACS Appl. Mater. Interf*., 2013, **5**, 861-868.

17. N. C. Miller, S. Sweetnam, E. T. Hoke, R. Gysel, C. E. Miller, J. A. Bartelt, X. Xie, M. F. Toney and M. D. McGehee, *Nano Lett*., 2012, **12**, 1566-1570.

18. H. Yan, D. Li, C. He, Z. Wei, Y. Yang and Y. Li, *Nanoscale*, 2013, **5**, 11649-11656.

19. J.-H. Huang, Y.-S. Hsiao, E. Richard, C.-C. Chen, P. Chen, G. Li, C.-W. Chu and Y. Yang, *Appl. Phys. Lett*., 2013, **103**, 043304.

20. D. H. Wang, A. K. K. Kyaw, J.-R. Pouliot, M. Leclerc and A. J. Heeger, *Adv. Energy Mater.*, 2014, **4**, 1300835.

21. Q. Sun, F. Zhang, J. Wang, Q. An, C. Zhao, L. Li, F. Teng and B. Hu, *J. Mater. Chem. A*, 2015, **3**, 18432-18441.

22. Q. Sun, F. Zhang, Q. An, L. Li, J. Wang, M. Zhang, W. Wang, F. Teng and J. Zhang, *Org. Electron*., 2015, **24**, 30-36.

23. S. Zhang, M. A. Uddin, W. Zhao, L. Ye, H. Y. Woo, D. Liu, B. Yang, H. Yao, Y. Cui and J. Hou, *Polym Chem-Uk*, 2015, **6**, 2752-2760.

24. Y. Liu, F. Zhang, H. Dai, W. Tang, Z. Wang, J. Wang, A. Tang, H. Peng, Z. Xu and Y. Wang, *Sol. Energy Mater. Sol. C.*, 2013, **118**, 135-140.

25. M. C. Scharber, D. Mühlbacher, M. Koppe, P. Denk, C. Waldauf, A. J. Heeger and C. J. Brabec, *Adv. Mater*., 2006, **18**, 789-794.

26. Z. He, C. Zhong, X. Huang, W.-Y. Wong, H. Wu, L. Chen, S. Su and Y. Cao, Adv. Mater., 2011, **23**, 4636-4643.

27. L. Lu, W. Chen, T. Xu and L. Yu, *Nat. Commun*., 2015, **6**, 7327.

28. Q. An, F. Zhang, Q. Sun, J. Wang, L. Li, J. Zhang, W. Tang and Z. Deng, *J. Mater. Chem. A*, 2015, **3**, 16653-16662.

29. M. Kim, J.-H. Kim, H. H. Choi, J. H. Park, S. B. Jo, M. Sim, J. S. Kim, H. Jinnai, Y. D. Park and K. Cho, *Adv. Energy Mater.*, 2014, **4**, 1300612